Proceedings of the World Congress on Engineering 2013 Vol III,
WCE 2013, July 3 - 5, 2013, London, U.K.

# Free Convective Boundary-Layer Flow over a Vertical Truncated Cone in a Bidisperse Porous Medium

Ching-Yang Cheng

*Abstract*—**This work studies the free convection heat transfer from a vertical truncated cone in bidisperse porous media with constant wall temperature. The two-velocity two-temperature model is used to derive the governing equations. The effects of the inter-phase heat transfer parameter, the modified thermal conductivity ratio, and the permeability ratio on the heat transfer and flow characteristics have been studied. Results show an increase in the modified thermal conductivity ratio or the permeability ratio tends to increase the free convection heat transfer rate of the vertical truncated cone in bidisperse porous media.**

***Index Terms***—**free convection, bidisperse porous medium, truncated cone, boundary layer flow.**

## I. Introduction

THE applications of bidisperse porous medium are found in bidisperse absorbent for enhancing absorption performance, or bidisperse capillary wicks in a heat pipe for enhancing heat pipe heat transfer rate. There are a lot of papers on the natural or mixed convection of bidisperse porous media. Nield and Kuznetsov [1] studied the conjugate forced convection heat transfer in bi-disperse porous medium channel. Nield and Kuznetsov [2] used a two-velocity two-temperature model to study the forced convection in a channel for a bi-disperse porous medium. Nield and Kuznetsov [3] examined the problem about the onset of convection in a bidisperse porous medium. Nield and Kuznetsov [4] studied the effect of combined vertical and horizontal heterogeneity on the onset of convection in a bidisperse porous medium. Nield and Kuznetsov [5] studied the natural convection about a vertical plate embedded in a bidisperse porous medium. Rees et al. [6] studied the vertical free convective boundary-layer flow in bidisperse porous media. Straughan [7] studied the Nield-Kuznetsiv theory for convection in bidisperse porous media. Kumari and Pop [8] studied the mixed convection boundary layer flow past a horizontal circular cylinder embedded in a bidisperse porous medium. Grosan et al. [9] studied the problem of free convection in a square cavity filled with a bisisperse porous medium. Narasimhan and Reddy [10] studied the natural convection inside a bidisperse porous medium enclosure. Narasimhan and Reddy [11] examined the resonance of natural convection inside a bidisperse porous medium enclosure. Nield and Kuznetsov [12] studied the forced convection in a channel partly occupied in a bidisperse porous medium.

This work studies the free convection heat transfer from a vertical truncated cone in bidisperse porous media with uniform wall temperature. The two-velocity two-temperature formulation is used to derive the governing differential equations. The cubic spline collocation method is used to solve the boundary layer equations. The effects of the inter-phase heat transfer parameter, the modified thermal conductivity ratio, and the permeability ratio on the free convection heat transfer characteristics are studied. .

## II. Analysis

Consider the boundary layer flow due to free convection heat transfer from a vertical truncated cone of half angle $A$ embedded in a bidisperse porous medium. The origin of the coordinate system is placed at the vertex of the truncated cone, with $x$ being the coordinate along the surface of the cone measured from the origin and y being the coordinate perpendicular to the conical surface, as shown in Fig.1. The surface of the vertical cone is maintained at a constant temperature $T_w$, which is different from the porous medium temperature sufficiently far from the surface of the vertical truncated cone.

A bidisperse porous medium is a porous medium in which the solid phase is replaced by another porous medium. There are two phases, as shown in Fig. 2. One is the f-phase and the other is the p-phase. In a bidisperse porous medium, the fluid occupies all of the f-phase and a fraction of the p-phase. We denote the volume fraction of the f-phase by $\phi$ and the porosity within the p-phase by $\varepsilon$. Thus $1-\phi$ is the volume fraction of the p-phase, and the volume fraction of the

Manuscript received February 17, 2013; revised March 14, 2013.

This work was supported by the National Science Council of Republic of China under the grant no. NSC 100-2221-E-218-045.

Ching-Yang Cheng is with the Department of Mechanical Engineering, Southern Taiwan University of Science and Technology, Yungkang 71005, Taiwan (phone: +886-6-2683734; fax: +886-6-2895877; e-mail: cycheng@mail.stust.edu.tw).

bidisperse porous medium by the fluid is $\phi+(1-\phi)\varepsilon$. Here we denote $T_f$ and $T_p$ as the volume-averaged temperature of the f-phase and the p-phase respectively. The volume average of the temperature over the fluid is given by

$$T_F=\frac{\phi T_f+(1-\phi)\varepsilon T_p}{\phi+(1-\phi)\varepsilon} \tag{1}$$

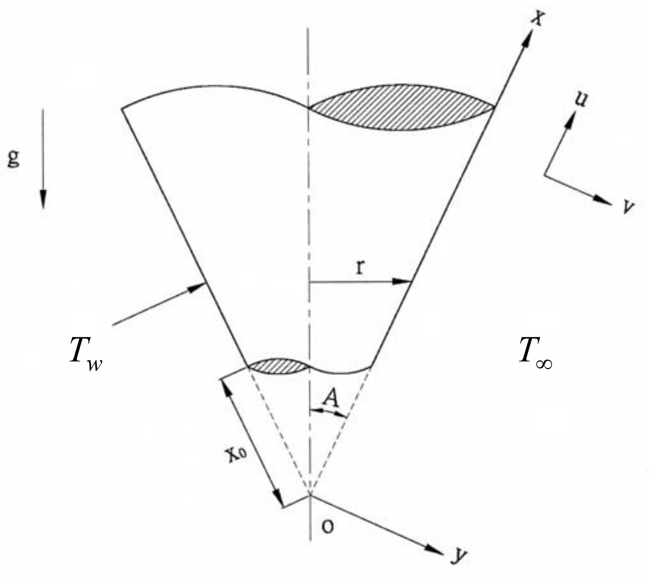


Fig. 1. Physical model and coordinates for a truncated cone.

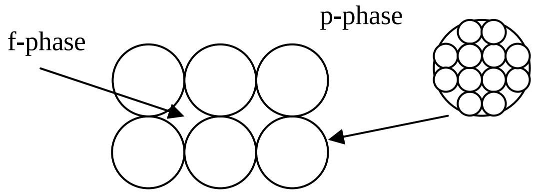


Fig. 2 Sketch of a bidisperse porous medium.

The fluid properties are assumed to be constant except for density variations in the buoyancy force term. The governing equations for the flow, heat transfer near the vertical cone can be written as [5, 13]

$$\frac{\partial(ru_f)}{\partial x}+\frac{\partial(rv_f)}{\partial y}=0 \tag{2}$$

$$\frac{\partial(ru_p)}{\partial x}+\frac{\partial(rv_p)}{\partial y}=0 \tag{3}$$

$$\frac{\mu}{K_f}\left(1+\frac{\varsigma K_f}{\mu}\right)\left(\frac{\partial u_f}{\partial y}-\frac{\partial v_f}{\partial x}\right)=\varsigma\left(\frac{\partial u_p}{\partial y}-\frac{\partial v_p}{\partial x}\right)$$

$$+\rho_F\beta_T g*\left(\frac{\partial T_F}{\partial y}\cos A+\frac{\partial T_F}{\partial x}\sin A\right) \tag{4}$$

$$\frac{\mu}{K_p}\left(1+\frac{\varsigma K_p}{\mu}\right)\left(\frac{\partial u_p}{\partial y}-\frac{\partial v_p}{\partial x}\right)=\varsigma\left(\frac{\partial u_f}{\partial y}-\frac{\partial v_f}{\partial x}\right)$$

$$+\rho_F\beta_T g*\left(\frac{\partial T_F}{\partial y}\cos A+\frac{\partial T_F}{\partial x}\sin A\right) \tag{5}$$

$$\phi(\rho c)_f\left(u_f\frac{\partial T_f}{\partial x}+v_f\frac{\partial T_f}{\partial y}\right)$$

$$=\phi k_f\left(\frac{\partial^2 T_f}{\partial x^2}+\frac{\partial^2 T_f}{\partial y^2}\right)+h(T_p-T_f) \tag{6}$$

$$(1-\phi)(\rho c)_p\left(u_p\frac{\partial T_p}{\partial x}+v_p\frac{\partial T_p}{\partial y}\right)$$

$$=(1-\phi)k_p\left(\frac{\partial^2 T_p}{\partial x^2}+\frac{\partial^2 T_p}{\partial y^2}\right)+h(T_f-T_p) \tag{7}$$

where $u_f$ and $v_f$ are the volume-averaged velocity components of the f-phase in the $x$ and $y$ directions. $u_p$ and $v_p$ are the volume-averaged velocity components of the p-phase in the the $x$ and $y$ directions. $K_f$ and $K_p$ are the permeabilities of the two phases, and $\varsigma$ is the coefficient for momentum transfer between the two phases. $\rho_F$ is the fluid density. $\beta_T$ is the volumetric thermal expansion coefficient of the fluid. $\mu$ is the viscosity of the fluid. Moreover, c is the specific heat at constant pressure and $k$ is the thermal conductivity. Moreover, $h$ is the inter-phase heat transfer coefficient, and $g*$ is the gravitational acceleration.

Because the boundary layer thickness is small, the local radius to a point in the boundary layer can be represented by the local radius of the vertical cone,

$$r=x\sin A \tag{8}$$

The boundary conditions for this problem are

$$y=0:\ T_f=T_w,\ T_p=T_w,\ v_p=0,\ v_f=0 \tag{9}$$

$$y\to\infty:\ T_f\to T_\infty,\ T_p\to T_\infty,\ u_p\to 0,\ u_f\to 0 \tag{10}$$

Here we introduce the stream functions, $\psi_f$ and $\psi_p$, to satisfy the relations:

$$u_f=\frac{1}{r}\frac{\partial\psi_f}{\partial y},\quad v_f=-\frac{1}{r}\frac{\partial\psi_f}{\partial x},\quad u_p=\frac{1}{r}\frac{\partial\psi_p}{\partial y},$$

$$v_p=-\frac{1}{r}\frac{\partial\psi_p}{\partial x} \tag{11}$$

Moreover, we define the nondimensional variables and parameters:

$$\bar{x}=\frac{x-x_0}{x_0},\quad \bar{y}=\frac{y}{x_0},\quad \bar{r}=\frac{r}{x_0},\quad \bar{\psi}_p=\frac{(\rho c)_p}{(1-\phi)k_p x_0}\psi_p,$$

$$\bar{\psi}_f=\frac{(\rho c)_f}{\phi k_f x_0}\psi_f,\ \theta_f=\frac{T_f-T_\infty}{T_w-T_\infty},\ \theta_p=\frac{T_p-T_\infty}{T_w-T_\infty} \tag{12}$$

Eqs. (2)-(7) become the following equations:

ISBN: 978-988-19252-9-9
ISSN: 2078-0958 (Print); ISSN: 2078-0966 (Online)

$$\frac{1+\sigma_f}{\bar{r}}\left(\frac{\partial^2\overline{\psi}_f}{\partial\bar{x}^2}+\frac{\partial^2\overline{\psi}_f}{\partial\bar{y}^2}-\frac{1}{1+\bar{x}}\frac{\partial\overline{\psi}_f}{\partial\bar{x}}\right)$$
$$-\frac{\beta\sigma_f}{\bar{r}}\left(\frac{\partial^2\overline{\psi}_p}{\partial\bar{x}^2}+\frac{\partial^2\overline{\psi}_p}{\partial\bar{y}^2}-\frac{1}{1+\bar{x}}\frac{\partial\overline{\psi}_p}{\partial\bar{x}}\right)$$
$$=Ra_l\left[\tau\frac{\partial\theta_f}{\partial\bar{y}}+(1-\tau)\frac{\partial\theta_p}{\partial\bar{y}}\right]+Ra_l\,tanA\left[\tau\frac{\partial\theta_f}{\partial\bar{x}}+(1-\tau)\frac{\partial\theta_p}{\partial\bar{x}}\right] \quad (13)$$

$$-\frac{\sigma_f}{\bar{r}}\left(\frac{\partial^2\overline{\psi}_f}{\partial\bar{x}^2}+\frac{\partial^2\overline{\psi}_f}{\partial\bar{y}^2}-\frac{1}{1+\bar{x}}\frac{\partial\overline{\psi}_f}{\partial\bar{x}}\right)$$
$$+\frac{\beta}{\bar{r}}\left(\frac{1}{K_r}+\sigma_f\right)\left(\frac{\partial^2\overline{\psi}_p}{\partial\bar{x}^2}+\frac{\partial^2\overline{\psi}_p}{\partial\bar{y}^2}-\frac{1}{1+\bar{x}}\frac{\partial\overline{\psi}_p}{\partial\bar{x}}\right)$$
$$=Ra_l\left[\tau\frac{\partial\theta_f}{\partial\bar{y}}+(1-\tau)\frac{\partial\theta_p}{\partial\bar{y}}\right]+Ra_l\,tanA\left[\tau\frac{\partial\theta_f}{\partial\bar{x}}+(1-\tau)\frac{\partial\theta_p}{\partial\bar{x}}\right] \quad (14)$$

$$\frac{\phi}{\bar{r}}\left(\frac{\partial\overline{\psi}_f}{\partial\bar{y}}\frac{\partial\overline{\theta}_f}{\partial\bar{x}}-\frac{\partial\overline{\psi}_f}{\partial\bar{x}}\frac{\partial\theta_f}{\partial\bar{y}}\right)$$
$$=\left(\frac{\partial^2\theta_f}{\partial\bar{x}^2}+\frac{\partial^2\theta_f}{\partial\bar{y}^2}\right)+H(\theta_p-\theta_f) \quad (15)$$

$$\frac{\phi}{\bar{r}}\left(\frac{\partial\overline{\psi}_p}{\partial\bar{y}}\frac{\partial\theta_p}{\partial\bar{x}}-\frac{\partial\overline{\psi}_p}{\partial\bar{x}}\frac{\partial\theta_p}{\partial\bar{y}}\right)$$
$$=\left(\frac{\partial^2\theta_p}{\partial\bar{x}^2}+\frac{\partial^2\theta_p}{\partial\bar{y}^2}\right)+\gamma H(\theta_f-\theta_p) \quad (16)$$

where the Darcy-Rayleigh number based on the characteristic length $x_0$ and properties in the f-phase is given by

$$Ra_l=\frac{\rho_F g^*\beta_T K_f x_0(T_w-T_\infty)\cos A}{\mu\phi k_f/(\rho c)_f} \quad (17)$$

Moreover, the modified thermal capacity ratio, the f-phase momentum transfer parameter, the porosity parameter, permeability ratio, the modified thermal conductivity ratio, and the inter-phase heat transfer parameter are respectively defined as

$$\beta=\frac{(1-\phi)k_p(\rho c)_f}{\phi k_f(\rho c)_p},\quad \sigma_f=\frac{\varsigma K_f}{\mu},\quad \tau=\frac{\phi}{\phi+(1-\phi)\varepsilon},$$
$$K_r=\frac{K_p}{K_f},\ \gamma=\frac{\phi k_f}{(1-\phi)k_p},\ H=\frac{hx_0^2}{\phi k_f} \quad (18)$$

The associated boundary conditions are given by

$$\bar{y}=0:\ \overline{\psi}_f=0,\ \overline{\psi}_p=0,\ \theta_f=1,\ \theta_p=1 \quad (19)$$

$$\bar{y}\to\infty:\ \frac{\partial\overline{\psi}_f}{\partial\bar{y}}\to 0,\ \frac{\partial\overline{\psi}_p}{\partial\bar{y}}\to 0,\ \theta_f\to 0,\ \theta_p\to 0 \quad (20)$$

Here we use the coordinate transformation given by

$$\tilde{x}=x,\ \tilde{y}=Ra_l^{1/2}\bar{y},\ \tilde{r}=\bar{r},\ \tilde{\psi}_f=Ra_l^{-1/2}\overline{\psi}_f,$$
$$\tilde{\psi}_p=Ra_l^{-1/2}\overline{\psi}_p \quad (21)$$

Table 1. Comparison of values of $-\theta'_{mp}\big|_{\eta=0}$ for free convection heat transfer from a vertical plate with constant wall temperature in mono-disperse porous media.

| $-\theta'_{mp}\big\|_{\eta=0}$ | | |
|---|---|---|
| Cheng and Minkowycz [15] | Rees and Pop [16] | Present |
| 0.4440 | 0.44378 | 0.4442 |

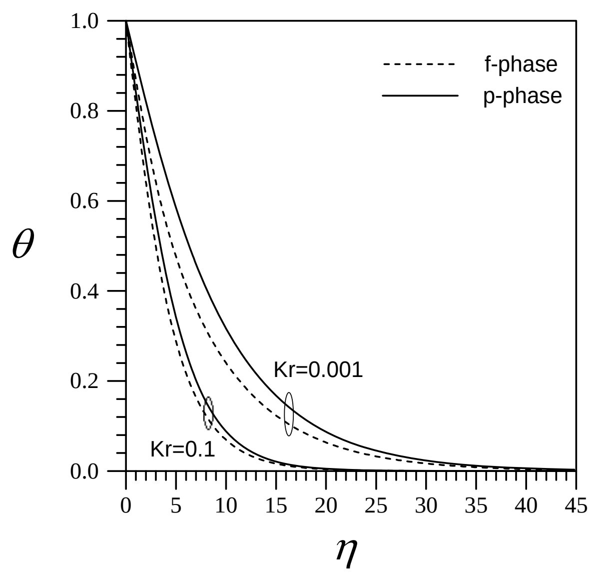


Fig. 3 The effect of the permeability ratio on the temperature profiles for the f-phase and the p-phase for $\xi=0.5$, $H=0.6$, $\beta=1$, $\gamma=0.2$, $\sigma_f=0.01$, $\phi=0.2$, $\varepsilon=0.4$, and $\tau=0.3846$.

Substituting Eq. (21) into Eqs. (13)-(16) and using boundary- layer approximation, we can obtain the following boundary-layer equations:

$$\frac{1+\sigma_f}{\tilde{r}}\frac{\partial^2\tilde{\psi}_f}{\partial\tilde{y}^2}-\frac{\beta\sigma_f}{\tilde{r}}\frac{\partial^2\tilde{\psi}_p}{\partial\tilde{y}^2}=\tau\frac{\partial\theta_f}{\partial\tilde{y}}+(1-\tau)\frac{\partial\theta_p}{\partial\tilde{y}} \quad (22)$$

$$-\frac{\sigma_f}{\tilde{r}}\frac{\partial^2\tilde{\psi}_f}{\partial\tilde{y}^2}+\frac{\beta}{\tilde{r}}\left(\frac{1}{Kr}+\sigma_f\right)\frac{\partial^2\tilde{\psi}_p}{\partial\tilde{y}^2}$$
$$=\tau\frac{\partial\theta_f}{\partial\tilde{y}}+(1-\tau)\frac{\partial\theta_p}{\partial\tilde{y}} \quad (23)$$

$$\frac{\partial^2\theta_f}{\partial\tilde{y}^2}-H(\theta_f-\theta_p)=\frac{\phi}{\tilde{r}}\left(\frac{\partial\tilde{\psi}_f}{\partial\tilde{y}}\frac{\partial\theta_f}{\partial\tilde{x}}-\frac{\partial\tilde{\psi}_f}{\partial\tilde{x}}\frac{\partial\theta_f}{\partial\tilde{y}}\right) \quad (24)$$

$$\frac{\partial^2\theta_p}{\partial y^2}-\gamma H(\theta_p-\theta_f)=\frac{\phi}{\tilde{r}}\left(\frac{\partial\tilde{\psi}_p}{\partial\tilde{y}}\frac{\partial\theta_p}{\partial\tilde{x}}-\frac{\partial\tilde{\psi}_p}{\partial\tilde{x}}\frac{\partial\theta_p}{\partial\tilde{y}}\right) \quad (25)$$

We may reduce Eqs. (22)-(25) to a form more convenient for numerical solution by the transformation:

ISBN: 978-988-19252-9-9
ISSN: 2078-0958 (Print); ISSN: 2078-0966 (Online)

$$\xi = \tilde{x} \quad , \quad \eta = \tilde{y} / \xi^{1/2} \quad , \quad \tilde{\psi}_p = \tilde{r}\xi^{1/2} g(\xi,\eta) \quad ,$$
$$\tilde{\psi}_f = \tilde{r}\xi^{1/2} f(\xi,\eta) \tag{26}$$

Substituting Eq. (26) into Eqs. (22)-(25), we obtain the following equations:

$$(1+\sigma_f)f' - \beta\sigma_f g' = \tau\theta_f + (1-\tau)\theta_p \tag{27}$$

$$-\sigma_f f' + \beta(K_r^{-1} + \sigma_f)g' = \tau\theta_f + (1-\tau)\theta_p \tag{28}$$

$$\theta_f'' + \left(\frac{1}{2} + \frac{\xi}{1+\xi}\right)\phi f\theta_f' - H\xi(\theta_f - \theta_p)$$
$$= \phi\xi\left(f'\frac{\partial\theta_f}{\partial\xi} - \theta_f'\frac{\partial f}{\partial\xi}\right) \tag{29}$$

$$\theta_p'' + \left(\frac{1}{2} + \frac{\xi}{1+\xi}\right)(1-\phi)g\theta_p' - \gamma H\xi(\theta_p - \theta_f)$$
$$= (1-\phi)\xi\left(g'\frac{\partial\theta_p}{\partial\xi} - \theta_p'\frac{\partial g}{\partial\xi}\right) \tag{30}$$

where primes denote differentiation with respect to $\eta$. Note that the momentum equations have been integrated once about $\eta$ to obtain Eqs. (27) and (28).

The boundary conditions are transformed to

$$\eta = 0: \ f = 0, \ g = 0, \ \theta_f = 1, \ \theta_p = 1 \tag{31}$$

$$\eta \to \infty: \ f' \to 0, \ g' \to 0, \ \theta_f \to 0, \ \theta_p \to 0 \tag{32}$$

Moreover, the local Nusselt numbers for the f-phase and the p-phase can be derived as

$$\frac{Nu_f}{\sqrt{Ra_x}} = -\theta_f'(\xi,0) \tag{33}$$

$$\frac{Nu_p}{\sqrt{Ra_x}} = -\theta_p'(\xi,0) \tag{34}$$

where $Nu_f = h_f x / k_f$ and $Nu_p = h_p x / k_p$. Note that $h_f$ and $h_p$ are the convection heat transfer coefficient for the f-phase and the p-phase. The Darcy-Rayleigh number based on the streamwise coordinate $x$ and properties in the f-phase is given by

$$Ra_x = \frac{\rho_F g^* \beta_T (T_w - T_\infty) K_f x}{\mu\phi k_f / (\rho c)_f} \tag{35}$$

## III. Results and Discussion

The transformed governing partial differential equations, Eqs. (29) and (30), and the associated boundary conditions, Eqs. (31) and (32), can be solved by the cubic spline collocation method [14]. The velocities $f'$ and $g'$ are calculated from the momentum equations, Eqs. (27) and (28). Moreover, the Simpson's rule for variable grids is used to calculate the values of $f$ and $g$ at every position from the boundary conditions, Eqs. (31) and (32). At every position, the iteration process continues until the convergence criterion for all the variables, $10^{-6}$, is achieved. Variable grids with 350 grid points are used in the $\eta$-direction. The optimum value of boundary layer thickness is used. Moreover, the backward finite difference is used to calculate the derivative about the streamwise coordinate $\xi$. To assess the accuracy of the solution, the present results are compared with the results obtained by other researchers. Table 1 shows the numerical values of $-\theta_{mp}'\big|_{\eta=0}$ for free convection heat transfer of a vertical smooth plate in mono-disperse porous media with constant wall temperature. The present results are in excellent agreement with the results reported by Cheng and Minkowycz [15] and Rees and Pop [16].

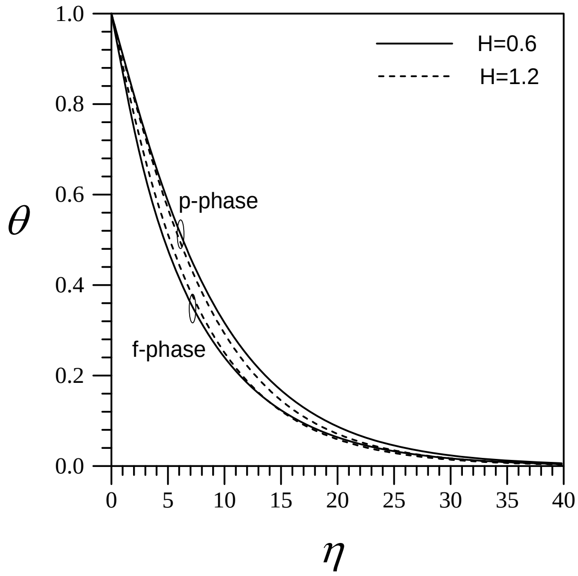


Fig. 4 The effect of the inter-phase heat transfer parameter on the temperature profiles for the f-phase and the p-phase for $\xi = 0.5$, $K_r = 0.001$, $\beta = 1$, $\gamma = 0.2$, $\sigma_f = 0.01$, $\phi = 0.2$, $\varepsilon = 0.4$, and $\tau = 0.3846$.

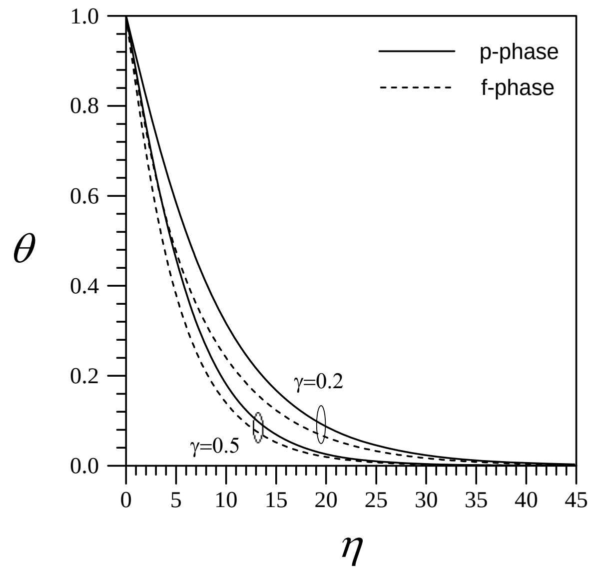


Fig. 5 The effect of the modified thermal conductivity ratio on the temperature profiles for the f-phase and the p-phase for $\xi = 0.5$, $H = 0.6$, $K_r = 0.001$, $\beta = 1$, $\sigma_f = 0.01$, $\phi = 0.2$, $\varepsilon = 0.4$, and $\tau = 0.3846$.

ISBN: 978-988-19252-9-9
ISSN: 2078-0958 (Print); ISSN: 2078-0966 (Online)

Fig. 3 shows the effect of the permeability ratio *Kr* on the temperature profiles for the f-phase and the p-phase. As the permeability ratio is increased, both the boundary layers of the solid phase and the fluid phase become thinner, thus increasing the temperature gradients of the f-phase and the p-phase. Moreover, a decrease in the permeability ratio tends to increase the temperature difference between the f-phase and the p-phase, thus enhancing the thermal non-equilibrium effect.

Fig. 4 shows the effect of the inter-phase heat transfer parameter $H$ on the temperature profiles for the f-phase and the p-phase. Results show that a decrease in the inter-phase heat transfer parameter tends to increase the temperature difference between the f-phase and the p-phase, thus enhancing the thermal non-equilibrium effect. In other words, when the inter-phase heat transfer parameter is small, the temperature field corresponding to the p-phase occupies a much greater region than does the temperature field of the f-phase.

Fig. 5 shows the effect of the modified thermal conductivity ratio $\gamma$ on the temperature profiles for the f-phase and the p-phase. As the modified thermal conductivity ratio is increased, both the boundary layers of the solid phase and the fluid phase become thinner, thus increasing the temperature gradients of the f-phase and the p-phase. Moreover, decreasing the modified thermal conductivity ratio increases the temperature difference between the f-phase and p-phase, thus enhancing the thermal non-equilibrium effect.

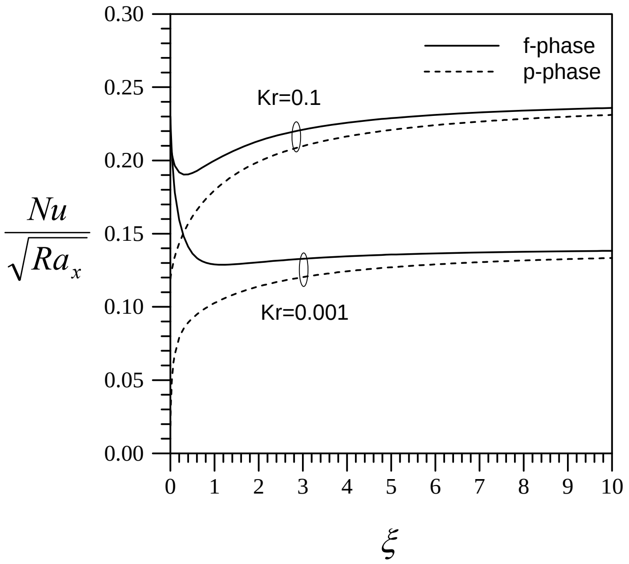


Fig. 6 The effect of the permeability ratio on the local Nusselt numbers for the f-phase and the p-phase for $H = 0.6$, $\beta = 1$, $\gamma = 0.2$, $\sigma_f = 0.01$, $\phi = 0.2$, $\varepsilon = 0.4$, and $\tau = 0.3846$.

Fig. 6 shows the effect of the permeability ratio $K_r$ on the local Nusselt numbers for the f-phase and the p-phase. Results show that an increase in the permeability ratio tends to increase both the local Nusselt numbers for the f-phase and the p-phase. In other words, the heat transfer rate for the bidisperse porous medium can be effectively increased by raising the permeability ratio. Moreover, with smaller coordinates, the local Nusselt number for the f-phase is much higher than that for the p-phase. The two phases are in the state of thermal non-equilibrium. As the streamwise coordinate is increased, the local Nusselt number for the f-phase approaches that for the p-phase. The bidisperse porous medium gradually approaches the state of thermal equilibrium far downstream.

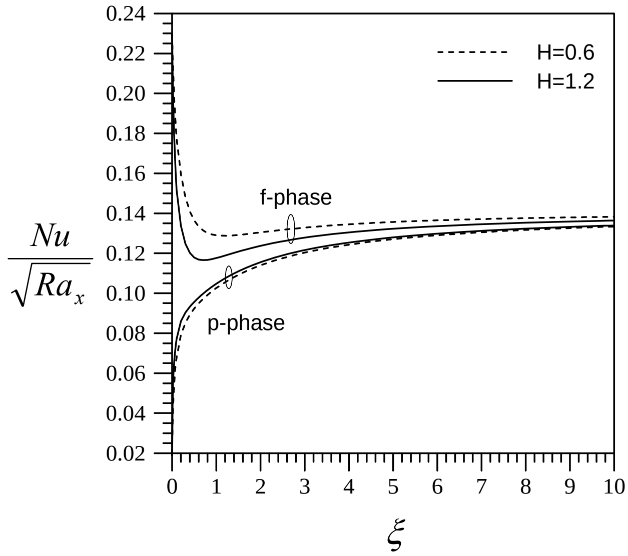


Fig. 7 The effect of the inter-phase heat transfer parameter on the local Nusselt numbers for the f-phase and the p-phase for $K_r = 0.001$, $\beta = 1$, $\gamma = 0.2$, $\sigma_f = 0.01$, $\phi = 0.2$, $\varepsilon = 0.4$, and $\tau = 0.3846$.

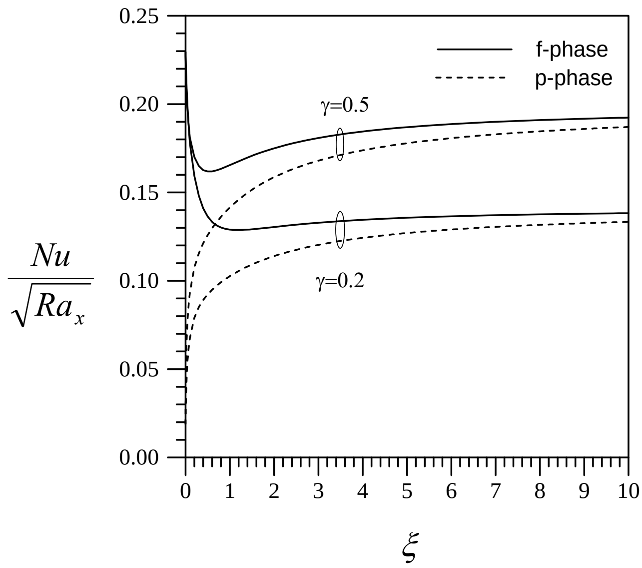


Fig. 8 The effect of the modified thermal conductivity ratio on the local Nusselt numbers for the f-phase and the p-phase for $H = 0.6$, $K_r = 0.001$, $\beta = 1$, $\sigma_f = 0.01$, $\phi = 0.2$, $\varepsilon = 0.4$, and $\tau = 3846$.

Fig. 7 shows the effect of the inter-phase heat transfer parameter $H$ on the local Nusselt numbers for the f-phase and the p-phase. For a vertical truncated cone, decreasing the inter-phase heat transfer parameter tends to increase the difference between local Nusselt numbers for the f-phase and the p-phase. In other words, lower values of the inter-phase heat transfer parameter leads to the state of thermal non-equilibrium between the p-phase and the f-phase of the bidisperse porous medium.

ISBN: 978-988-19252-9-9
ISSN: 2078-0958 (Print); ISSN: 2078-0966 (Online)

Fig. 8 shows the effect of the modified thermal conductivity ratio $\gamma$ on the local Nusselt numbers for the f-phase and the p-phase. For a vertical truncated cone, an increase in the modified thermal conductivity ratio $\gamma$ tends to increase both the local Nusselt number for the f-phase and local Nusselt number for the p-phase. In other words, the heat transfer rate for the bidisperse porous medium can be effectively increased by raising the modified thermal conductivity ratio.

## IV. CONCLUSION

This work has studied the free convection heat transfer from a vertical truncated cone embedded in bidisperse porous media with constant wall temperature. This work uses the two-velocity two-temperature model and the coordinate transformation to obtain the boundary layer equations. The cubic spline collocation method is used to solve the boundary layer equations. The effects of the inter-phase heat transfer parameter, the modified thermal conductivity ratio, and the permeability ratio on the free convection heat transfer characteristics have been studied. Results show an increase in the modified thermal conductivity ratio or the permeability ratio tends to increase the free convection heat transfer rate of the vertical truncated cone in bidisperse porous media. Moreover, an increase in the inter-phase heat transfer parameter tends to enhance the thermal non-equilibrium effect between the p-phase and the f-phase of the bidisperse porous medium.

## REFERENCES

[1] D.A. Nield and A. V. Kuznetsov, “Forced Convection in Bi-disperse Porous Medium Channel: a Conjugate Problem,” *International Journal of Heat and Mass Transfe*, vol.47, pp. 5375-5380, 2004.

[2] D.A D.A. Nield and A. V. Kuznetsov, “A Two-velocity Two-temperature Model for a Bi-disperse Porous Medium: Forced Convection in a Channel,” *Transport in Porous Media*, vol.59, pp. 325-339, 2005.

[3] D.A. Nield and A. V. Kuznetsov, “The Onset of Convection in a Bidisperse Porous Medium,” *International Journal of Heat and Mass Transfer*, vol.49, pp. 3068-3074, 2006.

[4] D. A. Nield and A. V. Kuznetsov, “The Effect of Combined Vertical and Horizontal Heterogeneity on the Onset of Convection in a Bidisperse Porous Medium,” *International Journal of Heat and Mass Transfer*, vol.50, pp. 3329-3339, 2007.

[5] D. A. Nield and A. V. Kuznetsov, “Natural Convection about a Vertical Plate Embedded in a Bidisperse Porous Medium,” *International Journal of Heat and Mass Transfer*, vol.51, pp. 1658-1664, 2008.

[6] D.A.S. Rees, D.A. Nield, and A. V. Kuznetsov, “Vertical Free Convective Boundary-layer Flow in a Bidisperse Porous Medium,” *ASME Journal of Heat Transfer*, vol.130, pp. 092601.1-092601.9, 2008.

[7] B. Straughan, “On the Nield-Kuznetsiv Theory for Convection in Bidisperse Porous Media,” *Transport in Porous Media,* vol.77, pp. 159-168, 2009.

[8] Kumari, M. and Pop, I., “Mixed Convection Boundary Layer Flow past a Horizontal Circular Cylinder Embedded in a Bidisperse Porous Medium,” *Transport in Porous Media*, vol.77, pp.287-303, 2009.

[9] T. Grosan, I. Pop, and D. B. Ingham, “Free Convection in a Square Cavity Filled with a Bidisperse Porous Medium,” *International Journal of Thermal Sciences,* vol.48, pp.1876-1883, 2009.

[10] A. Narasimhan and B.V.K. Reddy, “Natural Convection Inside a Bidisperse Porous Medium Enclosure,” *ASME Journal of Heat Transfer*, Vol.132, pp. 012502.1-012502.9, 2010.

[11] A. Narasimhan and B.V.K. Reddy, “Resonance of Natural Convection inside a Bidisperse Porous Medium Enclosure,” *ASME Journal of Heat Transfer*, vol.133, pp. 042601.1-042601.9, 2011.

[12] D. A. Nield and A. V. Kuznetsov, “Forced Convection in a Channel Partly Occupied in a Bidisperse Porous Medium: Symmetric Case,” *ASME Journal of Heat Transfer*, vol.133, pp. 072601.1-072601.9, 2011.

[13] K. A. Yih, “Coupled Heat and Mass Transfer by Free Convection over a Truncated Cone in Porous Media: VWT/VWC or VHF/VMF,” *Acta Mechanica,* vol.137, pp.83-97, 1999.

[14] P. Wang and R. Kahawita, “Numerical Integration of a Partial Differential Equations Using Cubic Spline,” *International Journal of Computers and Mathematics*, vol.13, pp. 271-286, 1983.

**[15]** P. Cheng, W.J. Minkowycz, “Free Convection about a Vertical Plate Embedded in a Porous Medium with Application to Heat Transfer from a Dyke,” *Journal of Geophysics Research*, vol. 82, pp. 2040-2044, 1977.

**[16]** D.A.S. Rees, I. Pop, “Vertical Free Convective Boundary-layer Flow in a Porous Medium Using a Thermal Nonequilibrium Model,” *Journal of Porous Media,* vol. 3, pp. 31-44, 2000.

ISBN: 978-988-19252-9-9
ISSN: 2078-0958 (Print); ISSN: 2078-0966 (Online)